Available online at www.sciencedirect.com
SCIENCE DIRECT
Journal of Photochemistry and Photobiology A: Chemistry 180 (2006) 101–108
Journal of Photochemistry and Photobiology A:Chemistry
www.elsevier.com/locate/jphotochem

Unusual conformational effects in proton transfer kinetics of an excited photochromic Schiff base

Marcin Ziółek [a,*], Jacek Kubicki [b], Andrzej Maciejewski [a,c], Ryszard Naskręcki [b], Wojciech Łuniewski [d], Anna Grabowska [e]

[a] *Center for Ultrafast Laser Spectroscopy, Adam Mickiewicz University, Umultowska 85, 61-614 Poznan, Poland*
[b] *Quantum Electronics Laboratory, Faculty of Physics, Adam Mickiewicz University, Umultowska 85, 61-614 Poznan, Poland*
[c] *Photochemistry Laboratory, Faculty of Chemistry, Adam Mickiewicz University, Grunwaldzka 6, 60-780 Poznan, Poland*
[d] *Pharmaceutical Research Institute, Rydygiera 8, 01-793 Warsaw, Poland*
[e] *Institute of Physical Chemistry, Polish Academy of Sciences, Kasprzaka 44, 01-224 Warsaw, Poland*

Received 21 June 2005; received in revised form 3 October 2005; accepted 3 October 2005
Available online 7 November 2005

Abstract

The compound 4-methoxy-2,5-bis(phenyliminomethyl)-phenol representing a group of recently synthesized new photochromic Schiff bases, has been studied by transient absorption and time-resolved fluorescence measurements in femto- and picosecond time domains. Two different conformers of the keto tautomer, decaying with the time constants 480 and 110 ps, have been detected. The first one is created within 50 fs, and the second one – exceptionally slowly – with the time constant of about 10 ps. The fast route occurs in the planar system, and the slow one involves the rotation around the C–C bond between the central phenyl ring and the phenylimino group, leading to the metastable photochromic form. For the first keto conformer the evidence of fast vibrational relaxation taking place on the time scale of several hundreds of femtoseconds is observed.

Keywords: Excited state intramolecular proton transfer; Photochromism; Schiff bases; Ultrafast laser spectroscopy

1. Introduction

The aromatic hydrogen bonded Schiff bases represent a special group of molecular systems in which two interesting phenomena occur: the excited state intramolecular proton transfer (ESIPT) and photochromism, being of great interest from the academic point of view as well as because of their various applications [1–3]. Recently, much progress has been made in the understanding of the ESIPT reaction. The analysis of transient absorption measured in the visible and infrared spectral ranges of probing wavelength together with detailed theoretical calculations indicate that the proton transfer occurs in the time range up to 100 fs for a large class of molecules with intramolecular hydrogen bonding [4–10]. The proton transfer time constants were determined on the basis of rate equation analysis as the rise time of the signal from the proton-transferred form [4–6] or from the time delay of the instantaneous rise of that signal [7,8,10]. The time scale of ESIPT correlates very well with the half-period of the observed oscillatory components in the measured signals [5,7–10] identified as the low frequency skeletal vibrations of molecules.

In Schiff bases not only the ESIPT reaction takes place upon excitation, but at least two transient species are observed: the keto tautomer exhibiting largely bathochromically shifted fluorescence, and the long lived photochromic transient in the ground state, created from the electronically excited keto form after structural changes. Earlier, we have studied the photophysics of salicylideneaniline (SA) [11], the best known photochromic Schiff base [12–19], and a much larger molecule, bis(salicylidene)-*p*-phenylenediamine (BSP) [20]. Both molecules were observed to undergo an extremely fast proton transfer reaction, with characteristic times within 50 fs.

In the present work we focus our attention on the recently synthesized Schiff base, 4-methoxy-2,5-bis(phenyliminomethyl)-phenol (BPHMe) [21], shown in Scheme 1. It is a monomethoxy-

* Corresponding author. Tel.: +48 61 829 5011.
E-mail address: marziol@amu.edu.pl (M. Ziółek).

1010-6030/$ – see front matter © 2005 Elsevier B.V. All rights reserved.
doi:10.1016/j.jphotochem.2005.10.001

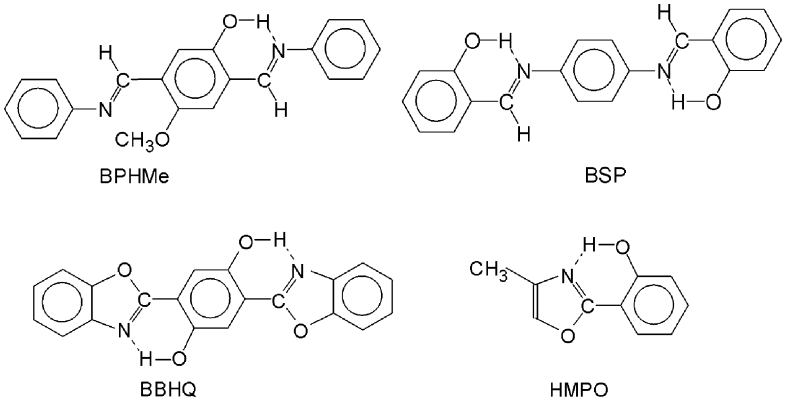

Scheme 1. Formulae of the molecules studied or discussed in this paper.

derivative of the bis(phenyliminomethyl)hydroquinone (BPH), which is isomeric to BSP. However, unlike BSP, here the proton donating OH substituents are localized in the central phenyl ring. There are at least two reasons why we are interested in the monomethoxy derivative of the BPH and not on BPH itself. The first is that as shown earlier [14,15] in symmetric Schiff bases, like BSP and BPH, the proton transfer reactivity is localized on only one salicylidene subunit, so the monomethoxy-derivative represents well the primary system, and the second is that for the monomethoxy-derivative much stronger fluorescence and transient absorption signals are observed making the results much more reliable [21]. The aim of the present study was to resolve the ultrafast stages of the early events leading to the creation of the keto tautomer and – eventually – to photochromic form.

The stationary absorption and emission spectra of BPHMe together with time resolved transient absorption from nano- to microsecond time scale were measured in acetonitrile (ACN) as a polar, aprotic solvent [21]. In the above work the decay time of the keto tautomer and the creation of the ground state of the photochromic transient was equal to about 0.3 ns (close to the limit of the temporal resolution of the apparatus). The lifetime of the latter was measured as about 1.2 ms. In our work we combine the data of transient absorption in femto- and picosecond time range with the picosecond time-resolved fluorescence in ACN in order to investigate the mechanism, dynamics and efficiency of ESIPT reaction and keto tautomer formation.

In some respect BPHMe is structurally similar to the widely studied system, 2,5-bis(benzoxazolyl)hydroquinone (BBHQ), possessing also in its framework a hydroquinone fragment [22–36], as shown in Scheme 1. BBHQ is a rare example of ESIPT compound, in which the dual fluorescence was measured in nonpolar solvents at room temperature [22,25,28–31] and after cooling in supersonic jets as well [23,32]. Interestingly enough, the short-wavelength enol fluorescence was not observed in van der Waals complexes and in low temperature matrices of noble gases [24,27,32]. The time resolved fluorescence measurements of BBHQ in *n*-heptane on the pico- and nanosecond time scale revealed the exceptionally low rate of intramolecular proton transfer of the order of $10^{10}\,s^{-1}$. Moreover, the equilibrium between the enol and keto tautomers, resulting from efficient back proton transfer, was observed [26,28,30]. Similar results were recently obtained for some derivatives of BBHQ [37]. However, in the recent femtosecond transient absorption studies of BBHQ in tetrahydrofuran the ESIPT reaction with the time constant of 110 fs was observed [35], together with the modulation of the signal by low frequency vibrational modes, characteristic of ultrafast proton transfer reactions [8–10]. Although for BBHQ the strong arguments in favour of the single proton transfer mechanism of tautomerization were delivered in the first publications [22,30,31,34], recently the existence of a double-proton transferred state in the isolated BBHQ molecule was suggested [36]. Therefore, the photophysics of "BBHQ family" of molecules is not fully understood and established yet.

2. Experimental

BPHMe was synthesized as described in [21] and additionally recrystallized from a mixture of hexane and methylene chloride. All measurements were performed at room temperature in dried ACN (for fluorescence, Merck, or anhydrous, Aldrich). The concentration of BPHMe was of about 1×10^{-4} M.

The equipments for stationary and time-resolved measurements were the same as described in our previous papers [11,20]. Briefly, the stationary UV–vis absorption spectra were measured with a UV–VIS-550 (Jasco) spectrophotometer. The steady-state fluorescence emission spectra were recorded with a FS900 spectrofluorimeter (Edinburgh Instruments) with a laser as an excitation source. The fluorescence excitation spectra were recorded with a modified MPF-3 (Perkin-Elmer) spectrofluorimeter [38]. This spectrofluorimeter was also used to measure the fluorescence quantum yields (ϕ_F), using quinine sulfate in 0.1 N sulfuric acid as the standard ($\phi_F = 0.53$) [39]. The apparatus used for time-resolved emission measurements (time correlated single photon counting, TCSPC) and for the transient absorption measurements was described in details earlier [40,41]. The repetition rate of the laser system for the time-resolved emission measurements (Ti:sapphire) was set at 4 MHz providing pulses of about 1 ps duration. The excitation wavelength was set at 400 nm, and the experiments were carried out at the magic angle conditions. The temporal resolution of the spectrofluorimeter was about 1 ps [40], and the spectral resolution was 8 nm.

The repetition rate of the laser system for the transient absorption measurements (Ti:sapphire) was set at 1 kHz, providing pulses of about 100 fs duration. The probe beam was the white light continuum generated in a 2 mm rotating calcium fluoride plate. The thickness of the flowing sample was 2 mm, the pump pulse energy was 20 μJ, and the FWHM of the pump beam diameter at the sample was 0.75 mm. The pump pulse wavelength was set at 400 nm. The measurements were performed at the magic angle conditions. All the spectra analyzed were corrected for chirp of white light continuum [42]. The pump-probe cross correlation function unaffected by the cell thickness was determined from the two-photon absorption in a very thin (150 μm) BK7 glass plate; its FWHM is 150 fs. The real instrumental function used for the convolution with the kinetic exponential functions was determined separately for each wavelength, taking into account the cell thickness, and hence the dispersion of the delay between the pump and the probe pulses (originating from different group velocities of pump and probe pulses in the sample) [43]. For example, the FWHM of the instrumental function at the probe wavelength 650 nm is broadened to the value of 250 fs. The transient absorption signals, originating from the pure solvent, were subtracted from the data collected [44]. The transient absorption measurements were performed in the spectral range of 330–730 nm and the temporal range of 0–100 ps.

3. Results

3.1. Stationary absorption and fluorescence

The stationary absorption, emission and fluorescence excitation spectra for BPHMe in ACN are shown in Fig. 1. The absorption spectrum is presented in the scale of the relative intensity I of the absorbed light, $I = 1–10^{-A}$ (where A is the absorbance) to permit a comparison with the fluorescence excitation spectra. The absorption band with a maximum at 24 600 cm^{-1} ($\varepsilon_{max} = 18\,500\ M^{-1}\ cm^{-1}$) is assigned to the transition $S_1 \leftarrow S_0$ (π, π^*). The emission spectrum (excitation wavelength $\lambda_{exc} = 400$ nm) is corrected for the sensitivity of the detection system. The dominant signal is the emission from the keto tautomer with a characteristic large Stokes' shift, but the short-wavelength emission from the primary excited enol form can be also detected (see inset in Fig. 1). The possibility that the short-wavelength emission might originate from the noise, the solvent itself or solvent impurities has been excluded by the subtraction of the spectrum measured in the same experimental conditions in pure solvent. The fluorescence quantum yield of the keto tautomer is 1.8×10^{-2}. The ratio of short-wavelength emission intensity ($\lambda < 500$ nm) to the long-wavelength emission intensity ($\lambda > 500$ nm) is 6×10^{-4}. Unfortunately this extremely week emission spectrum of the fast decaying enol form cannot be reliably extracted from the tail of the long-wavelength fluorescence of the keto tautomer. The fluorescence excitation spectra were performed for the long-wavelength emission and they are in a very good agreement with the long-wavelength part (>380 nm) of the absorption spectrum. The relative intensity of the excitation spectra is significantly lower than in the absorption spectrum for the transitions to higher electronic states (<380 nm), which was also observed for previously studied Schiff bases [11].

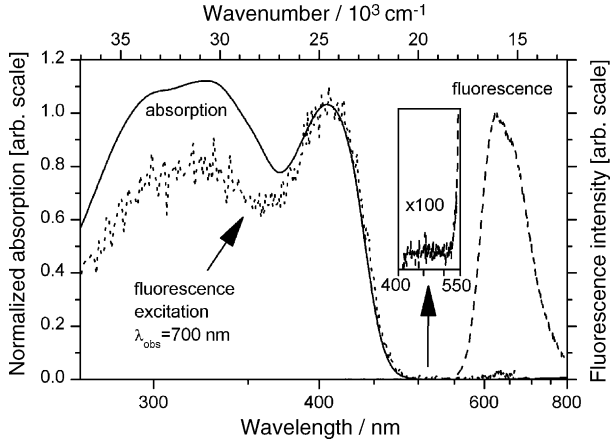

Fig. 1. The absorption, fluorescence ($\lambda_{exc} = 400$ nm) and fluorescence excitation spectra of BPHMe ($c = 1 \times 10^{-4}$ M) in ACN. The absorption spectrum is presented in the scale of the relative intensity of the absorbed light. The inset shows the 100 times magnified short-wavelength emission from the primary excited enol form. The fluorescence excitation spectra were the same for the other observation wavelengths in the long-wavelength emission range ($\lambda_{obs} > 570$ nm).

3.2. Time-resolved fluorescence

Dynamic emission measurements of BPHMe in ACN were performed for a number of emission wavelengths (λ_{em}) in the whole spectral range of emission. Because of the presence of Raman lines originating from the solvent, the measurements were performed for $\lambda_{em} > 460$ nm. The results of the two- or three-exponential fits are summarized in Table 1. For the

Table 1
A summary of kinetic parameters obtained by TCSPC method for the fluorescence of BPHMe in ACN

λ (nm)	a_1[a]	τ_1 (ps)[b]	a_2[c]	τ_2 (ps)[d]	a_3[c]	τ_3 (ps)[d]	χ^2
464	1.00	<1	<0.01	900 ± 500	–	–	0.95
500	1.00	4	<0.01	480 ± 300	–	–	0.96
550	0.72	8	0.18	448	0.10	92	0.98
560	0.45	15	0.37	490	0.18	144	1.04
575	0.14	14	0.69	485	0.17	160	1.00
590	−0.3	11	0.81	483	0.19	126	1.05
600	−0.9	9	0.84	484	0.16	130	1.01
610	−0.4	11	0.87	482	0.13	104	1.06
615	−0.9	9	0.86	483	0.14	106	1.02
620	−0.2	11	0.89	484	0.11	122	1.01
630	−0.3	11	0.87	484	0.13	104	1.03
640	−0.9	6	0.87	485	0.13	128	0.98
650	−0.9	6	0.88	485	0.12	131	1.05
675	−0.9	7	0.86	484	0.14	114	1.02
700	−0.9	6	0.87	485	0.13	118	1.03
725	−0.9	7	0.86	485	0.14	113	1.08
750	−0.7	7	0.87	484	0.13	96	0.99

The sum of amplitudes of decay components (positive amplitudes) is normalized to 1.
[a] ±0.01 (for λ ≤ 575 nm); ±0.4 (for λ ≥ 590 nm).
[b] ±5 ps.
[c] ±0.01.
[d] ±4 ps, except 464 and 500 nm.

short-wavelength emission kinetics (λ_{em} = 464 nm) the major part of the decay was identical to that of the instrument response function, hence the time of this decay was beyond the temporal resolution of the spectrofluorimeter used (<1 ps). For longer wavelengths (>550 nm), two components of the long decay times were obtained, equal to about 480 ps (major component) and 110 ps (minor component). The spectra associated with these two components are very similar. Besides, the third much shorter one of about 9 ps ($\pm$ 5 ps) was found: in the range of 500–575 nm it was present as the decay time (positive amplitude a_1), while for λ_{em} = 590 nm and longer wavelength it became a rise time (negative amplitude a_1). The pre-exponential factors in Table 1 were normalized so that the sum of the amplitudes of decay components (positive amplitudes) is equal to 1. For λ > 580 nm the component of instantaneous increase with amplitude $(1 + a_1)$ indicates that at least in some fraction of molecules the proton transfer reaction takes place in the ultrafast time scale. However, the fitting procedure revealed that the amplitude of the rise component and the rise time itself are strongly correlated with the "time zero" [27]. This is the reason why it is difficult to detect the short rise components [45]. The necessity of fitting the zero time origin is caused by the zero time drift (see Section VII.C in Ref. [40]). Thus, the ratio of the amplitudes of the slower (9 ps) rise time and the instantaneous (<1 ps) rise time $(-a_1/(1 + a_1)$ for λ_{em} > 575 nm) is uncertain. Fig. 2 presents the exemplary data at λ_{em} = 615 nm. The kinetic data were analyzed in terms of three possible fits: monoexponential decay, biexponential decay, and biexponential decay with one exponential rise. Both the weighted residuals distributions and χ^2 values (1.35, 1.13 and 1.03, respectively) clearly support the existence of three different components in the time-resolved emission. The reproducibility of the fits was checked by several independent measurements for selected wavelengths. The possibility that the rise component is due to the solvation can be excluded because the fitted rise time constant does not show any systematic changes with increasing wavelength.

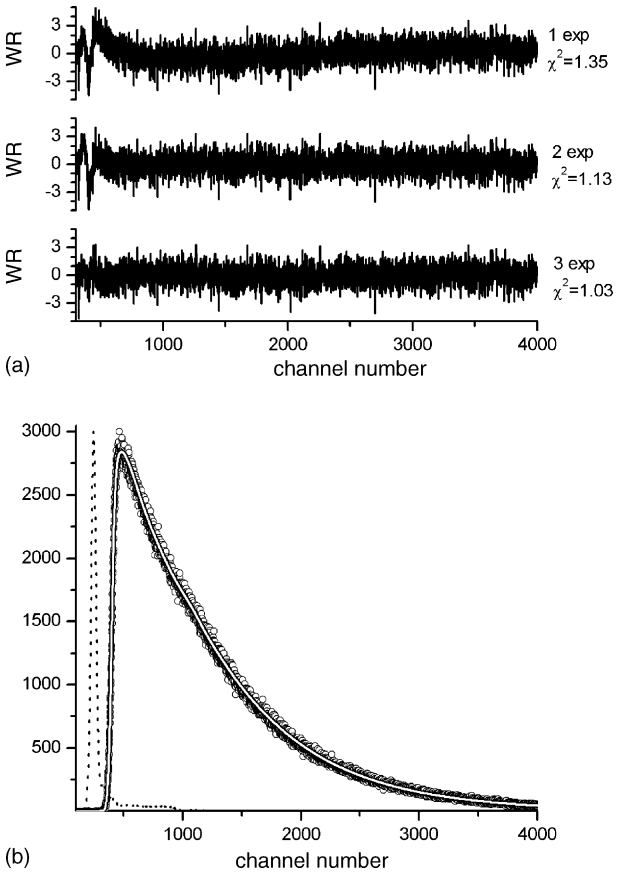

Fig. 2. The representative time resolved spontaneous emission data of BPHMe ($c = 1 \times 10^{-4}$ M) in ACN at λ_{em} = 615 nm (λ_{exc} = 400 nm). (a) Presents the weighted residuals distributions and χ^2 values for different fits assuming: one-exponential decay (1 exp, 471 ps), two-exponential decay (2 exp, 487 and 178 ps) and two-exponential decay with one-exponential rise (3 exp, 483 ps, 106 and 9 ps). (b) Presents the kinetics of the measured emission (open points), the best fit (black and white line) and the instrument response function profile (dotted line). For the sake of clarity the instrument response function was shifted to the left by 150 channels. One channel in the detection system corresponds to 0.61 ps.

3.3. Transient absorption

The transient absorption (ΔA) data for BPHMe in ACN are obtained from the spectra taken at about 90 different delay times. The reproducibility of the spectra was checked in three independent measurements. Fig. 3 presents exemplary spectra taken at delay times of −1, 0, 1.5 and 30 ps. To analyze the data, convolutions of two- or three-exponential decay with the instrumental function were fitted to the experimental kinetics recorded. The fits were performed every 5 nm in the whole spectral range (except for the range of 390–405 nm, disturbed by the pumping beam of 400 nm scattered in the direction of detection). Fig. 4 presents the kinetic curves for the most representative selected probe wavelengths.

Within the time of the instrumental function the amplitudes of the following bands rise: the ground state depopulation (GSD) in the spectral range below 430 nm (negative signal), the transient absorption in the spectral range from 430 to 600 nm (positive signal, with a maximum at 537 nm and a pronounced shoulder in the short-wavelength region) and the stimulated emission

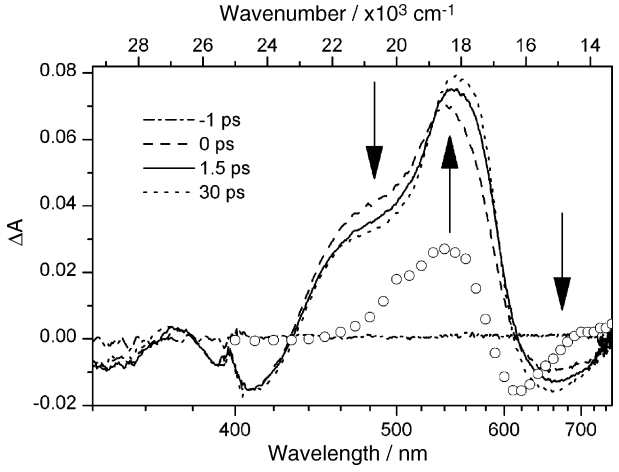

Fig. 3. Transient absorption spectra at selected delay times for BPHMe ($c = 1 \times 10^{-4}$ M) in ACN with the excitation of 400 nm. The arrows indicate the temporal changes of the spectra. For comparison the transient absorption spectrum of BBMP measured 150 ps after the excitation (from Ref. [31] after the renormalization) is shown as open points.

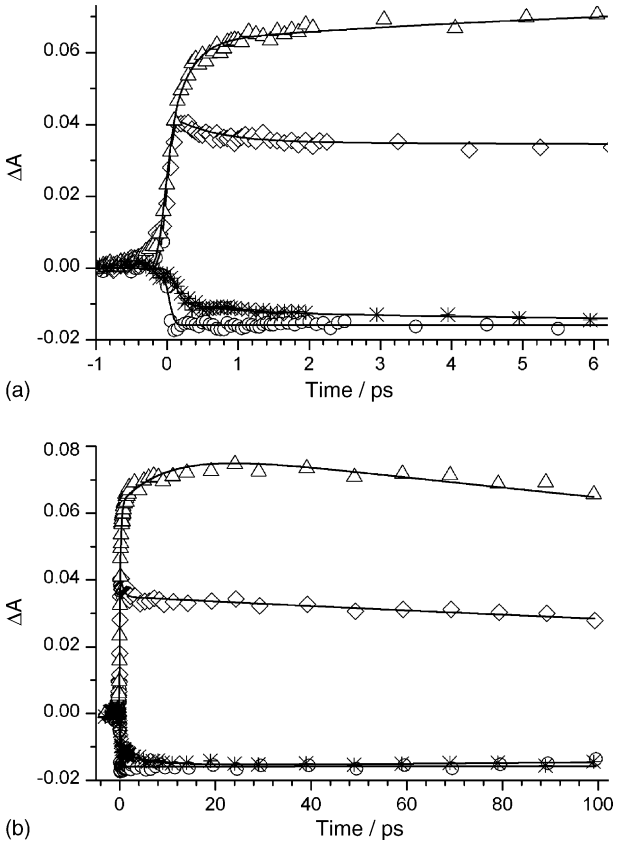

Fig. 4. Examples of the kinetic curves of the transient absorption signals for BPHMe in ACN, and the fits in the short (a) and long (b) time scale. The values of the fitted parameters (one-, two- or three-exponential functions convoluted with the instrumental function) are the following: 410 nm (circles): $A_1 = -0.015$, $\tau_1 = 10\,000$ ps; 480 nm (diamonds): $A_1 = 0.006$, $\tau_1 = 0.62$ ps, $A_2 = 0.035$, $\tau_2 = 450$ ps; 570 nm (triangles): $A_1 = -0.018$, $\tau_1 = 0.26$ ps, $A_2 = -0.018$, $\tau_2 = 10.2$ ps, $A_3 = 0.081$, $\tau_3 = 450$ ps; 650 nm (stars): $A_1 = 0.002$, $\tau_1 = 0.65$ ps, $A_2 = 0.004$, $\tau_2 = 7.2$ ps, $A_3 = -0.016$, $\tau_3 = 1500$ ps.

for wavelengths longer than 600 nm (negative signal), shown in Fig. 3. The GSD band corresponds to the ground state absorption of the primary enol form, while the stimulated emission occurs at the spectral region of the keto tautomer fluorescence. Both bands are modified by the presence of the strong transient absorption band between them. The instantaneous increase of the keto emission indicates that at least in some fraction of the molecules the proton transfer reaction takes place in the ultrafast time scale. Taking into account the temporal duration of our instrumental function we can only estimate the upper limit of this process as 50 fs (for longer rise times the increase of the keto emission would not be instantaneous). The same results were obtained in our previous studies of the molecules from the SA family [11,20].

Within the experimental error, the GSD signal remains constant in time (see kinetics for 410 nm in Fig. 4), which suggests that all excited molecules are transferred to the keto form with no indication of the return to the ground state of the primary enol form within first 100 ps after excitation. For wavelengths shorter than 400 nm the interplay between GSD and transient absorption together with lower signal to noise ratio made it impossible to obtain reliable kinetic fits.

The evolution of the transient absorption and the transient gain spectra in the short time range (up to ~30 ps) proceeds on two time scales: hundreds of femtoseconds (average value 500 ± 300 fs) and single picoseconds (average value 10 ± 5 ps). The faster component is observed as a decrease in transient absorption signal in the spectral range of 450–510 nm and as an increase in both, the absolute values of transient absorption in the range of 540–595 nm and stimulated emission for wavelength >630 nm (see Figs. 3 and 4a). Moreover, the spectral evolution of the transient absorption band is also accompanied by the time-dependent red shift of its maximum from 537 to 551 nm with similar time constants. The kinetic component of several picoseconds is observed as an additional increase in the transient absorption (540–595 nm) and stimulated emission (>630 nm) signals (see Figs. 3 and 4). The faster component could not be resolved in the time resolved fluorescence measurements, but the value of the longer one (10 ps) is in a very good agreement with the values of the shorter component in spontaneous emission (described in the previous section). In the further evolution (up to 100 ps) of transient absorption signals, a small decrease is observed, in agreement with the average value of the fluorescence decay time of the keto tautomer (about 400 ps = (0.8 × 480) + (0.2 × 110) ps). Such a decrease is also observed in the stimulated emission signal. The decay time constant fitted for particular wavelength (650 nm) in Fig. 4 is longer than expected, but it is probably due to the insufficient signal to noise ratio and too short time window. On the contrary, the GSD signal does not show any recovery, which suggests that all or almost all of excited molecules are transferred to the long lived (1.2 ms) ground state of the photochromic form. It should be also noted that it is impossible to distinguish the two 110 and 480 ps components (observed in the spontaneous emission kinetics) in the transient absorption data because the transient absorption experiments are carried out only up to 100 ps and the signal to noise ratio is worse than in the fluorescence TCSPC experiments.

4. Discussion

First, we wish to discuss the temporal changes of the transient absorption spectra proceeding on the short time scale. We assign the 500 fs component observed in the evolution of the transient absorption to the fast vibrational relaxation of the hot S_1 state of keto form, created after ultrafast (<50 fs) excited state proton transfer. This assignment is based on the observation of spectral narrowing and a shift of the maximum of the transient absorption signal, which are characteristic of such process. Indeed, in the central spectral range (540–595 nm) increase on the intensity is observed, while in the wings of the transient absorption band the signal decreases with the 500 fs time constant. In the short wavelength wing these changes are directly visible, while the long-wavelength wing is disturbed by the presence of stimulated emission band (the decrease in the transient absorption signal is correlated with the increase in the gain intensity). The strong evidence of vibrational relaxation is also consistent with the fact that the molecules under study are excited with relatively large amount of vibrational energy excess ~3500 cm^{-1} (excitation

400 nm). On the other hand the spectral narrowing and the shift of the transient absorption band were not observed when the molecules from "SA family" were excited at the longest possible wavelength [11]. However, these features were present when the excitation wavelength was much shorter [17]. In that case, the time scale of the spectral changes was also hundreds of femtoseconds. On the time scale of several hundreds of femtoseconds also the solvation dynamics might occur, which is manifested as a decrease in the blue part of the emission signal and an increase in the red part. However, in BPHMe such a mechanism does not explain the decrease in the transient absorption signal in the short wavelength region 450–510 nm (which would mean the increase in the blue part of the stimulated emission signal).

The longer component of the duration of about 10 ps is manifested as an additional rise in both the transient absorption and stimulated emission signals as well as an increase in the spontaneous fluorescence intensity from the S_1 keto state. Therefore, we attribute this 10 ps component to the creation of the second conformer of the keto tautomer in its S_1 state. The alternative, more commonly assumed explanation of the 10 ps component might be the solvent assisted vibrational cooling of the hot S_1 keto state. However, such a process should be accompanied by the spectral narrowing of the bands and is not consistent with our data since the 10 ps decay is absent in the short-wavelength wing of the transient absorption band and in the long-wavelength part of the emission spectrum (see Table 1). Moreover, the presence of two keto conformers with similar emission spectrum is strongly supported by the existence of two decay components in time resolved fluorescence measurements, 480 and 110 ps, which cannot be explained by the vibrational cooling.

There are three possible schemes of photoexcitation and deactivation involving the existence of two keto conformers. First, the two different conformers might already exist in the ground state of the primary enol form: in one of them the excited state proton transfer occurs in the ultrafast time scale of 50 fs, and in the second conformer the proton transfer is much slower, 10 ps. However, the existence of only one initial enol structure is indicated by the good agreement of the stationary fluorescence excitation spectra with the absorption spectrum. The theoretical calculations for BBHQ molecule also predict two keto conformers in S_1 state (planar and skewed), while the only stable enol structure is the planar one [32,36]. Another possibility is the creation of the second keto conformer from the first one in the time scale of 10 ps. Such a scheme, however, does not explain the features observed in the time-resolved spontaneous emission measurements: the two long decay components (480 and 110 ps) and the 10 ps decay in the spectral region 500–575 nm (between the enol and keto emission bands). The third explanation, which we consider the most probable one, is based on two different routes of excited state proton transfer reaction, and will be discussed below in more details.

Analysis of the wavelength dependence of the parameters describing the kinetics of the spontaneous emission signals (Table 1) reveals many similarities with the recent results of the up-conversion measurements of 2-(2′-hydroxyphenyl)-4-methyloxazole (HMPO) in *p*-dioxane [46]. HMPO also undergoes ESIPT reaction and its structure resembles that of a half of the BBHQ molecule (see Scheme 1). In the short-wavelength part of the emission (from the enol form of HMPO) a very fast 100 fs decay was observed, which corresponded to the <1 ps decay of BPHMe at 464 nm. In the spectral range between the enol and keto emission, the existence of a longer decay for HMPO (two components of 300 fs and 3 ps) corresponding to our 10 ps decay for BPHMe (from 500 to 575 nm) was detected. Finally, there was a bi-exponential increase (150 fs and 6 ps) in the emission intensity of the keto form of HMPO, while in our case the rise time component of about 10 ps was observed for the wavelength of 590 nm and longer. The authors of Ref. [46] interpreted their results as the evidence of two trajectories along which the proton transfer evolves: the ultrafast route corresponded to the barrierless mechanism between the planar structures of enol and keto form, while the slower process involved the twisting motion of two heterocyclic moieties of the HMPO molecule [47]. We think that such an explanation should be also valid in our case. Thus, the planar and twisted conformers in the S_1 keto state of BPHMe have one common precursor, which is the planar enol structure.

In conclusion, we propose the following deactivation scheme (Scheme 2). After the excitation of the planar enol form of BPHMe two competing processes occur on the ultrafast (<50 fs) time scale: the proton transfer (in which the planar keto conformer is created) and the twisting motion in the enol form. We think that the twist takes place around the C–C bond between the central phenyl ring and the phenylimino group (see Scheme 2), in analogy to HMPO [47]. The proton transfer process is manifested as the instantaneous increase in the stimulated and spontaneous emission signals of the keto tautomer. In the twisted enol much slower proton transfer with the rate constant of about $(10\,\text{ps})^{-1}$ takes place, leading to the twisted keto conformer. It is accompanied by the 10 ps decay of the spontaneous emission in the spectral region 500–575 nm (emission from the twisted enol rotamer is bathochromically shifted with respect to the planar one), the additional 10 ps rise of the stimulated and spontaneous emissions of the keto form as well as the additional increase in the transient absorption at the maximum of the keto band. In the transient absorption kinetics the amplitudes of the slower process are 15–25% of the total amplitudes, and the contribution of the 110 ps minor component in the long fluorescence lifetimes is similar. Therefore, it is highly probable that the lifetime of the dominant planar keto conformer is 480 ps while the twisted keto conformer decays with the time constant of 110 ps, both leading to the photochromic form. The twisted keto conformer is better prepared for the creation of photochrome, which is the *trans*-keto transient with the 180° rotation around the considered C–C bond (see Scheme 2) [21]. Thus, the lifetime of the twisted keto conformer is shorter than the lifetime of the planar one.

Now we would like to relate our measurements of BPHMe to the results of similar molecular systems. To our knowledge, in no other photochromic Schiff bases two different rise times of the keto tautomer emission have been found (only the decays). Moreover, the lifetimes of the S_1 states of the keto tautomers of BPHMe are more than an order of magnitude longer than

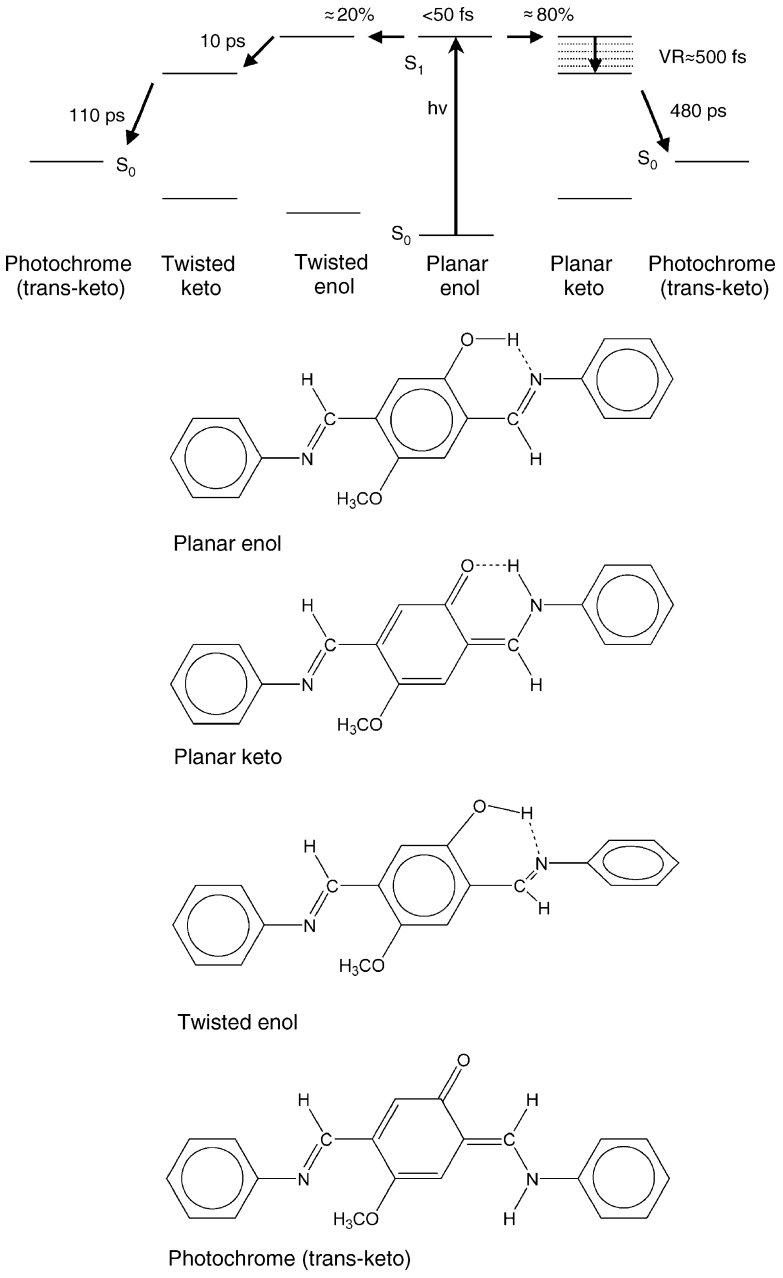

Scheme 2. Proposed deactivation scheme of BPHMe.

the corresponding lifetime of the BSP molecule (10.5 ps [20]), which belongs to the "SA family" (see Scheme 1). The probable explanation is that the internal hydrogen bond in the BPHMe molecule is localized in the central phenyl ring and might be stronger than in BSP [21]. Therefore, the keto tautomers of BPHMe are more stable than that of BSP assuming that the main deactivation channel of S_1 keto state in these molecules are structural changes (including the creation of photochromic form).

It is worth noting that the transient spectrum of keto form of BPHMe is similar to the corresponding absorption state of the monometoxy derivative of BBHQ (BBMP) [30,31] (see Fig. 3). Also, the radiative rate constants of the keto tautomers are comparable in both molecules, which also supports the close analogy of these two systems. Of course, in BBMP the photochromic transient cannot be created and the deactivation of the S_1 state of keto form takes place only via the slower channel of internal conversion.

The relatively slow proton transfer process in one of the conformers of BPHMe resembles the exceptionally low values of this reaction rate reported for BBHQ and BBMP [26,28,30]. Having in mind the recent report on a much faster ESIPT reaction observed for BBHQ in tetrahydrofuran (110 fs, [35]), we would like to propose the explanation of this controversy based on our studies of BPHMe. The temporal resolution of the instruments used for measurements described in Refs. [26,28,30] was of the order of picoseconds, while the studies reported in Ref. [35] were performed only up to 3 ps. Thus, perhaps in the molecules of the

"BBHQ family" compounds also two competing proton transfer processes take place, like in BPHMe: the ultrafast, observed in Ref. [35], and a slower one, seen in Refs. [26,28,30].

5. Conclusions

The time-resolved transient absorption and emission measurements on the pico- and femtosecond time scale as well as the stationary absorption and emission measurements of BPHMe molecule in ACN are presented. Two different conformers of the keto tautomer of this molecule are created: the first one within 50 fs, and the second one with the time constant of about 10 ps. For the first conformer the evidence of fast vibrational relaxation taking place on the time scale of several hundreds of femtoseconds is demonstrated. All molecules are transferred from the initial excited enol form to two keto tautomers which decay with the time constants of 480 and 110 ps. The most probable explanation is that these two conformers are the products of two different routes of the excited state proton transfer reaction. The investigated molecule is structurally closely related to two widely studied systems: "SA family" of Schiff bases and "BBHQ family" of hydroquinones. The similarities and differences in the photophysics of BPHMe and these systems are also discussed.

Acknowledgements

This work was performed under financial support of the KBN (State Committee for Scientific Research) project 2 P03B 015 24. Dynamics measurements were made at the Center for Ultrafast Laser Spectroscopy at the University of A. Mickiewicz in Poznan, Poland.

References

[1] T. Elsaesser, H.J. Bakker (Eds.), Ultrafast Hydrogen Bonding Dynamics and Proton Transfer Processes in the Condensed Phase, Kluwer Academic Publishers, Dordrecht, 2002.
[2] E. Hadjoudis, in: H. Dürr, H. Bouas-Laurent (Eds.), Photochromism: Molecules and Systems, Elsevier, Amsterdam, 1990, p. 685 (Chapter 17).
[3] Chem. Rev. 100 (2000) 5 (special issue on Photochromism: Memories and Switches).
[4] J.L. Herek, S. Pedersen, L. Banares, A.H. Zewail, J. Chem. Phys. 97 (1992) 9046–9061.
[5] C. Chudoba, E. Riedle, M. Pfeiffer, T. Elsaesser, Chem. Phys. Lett. 263 (1996) 622–628.
[6] T. Fournier, S. Pommeret, J.-C. Mialocq, A. Deflandre, R. Rozot, Chem. Phys. Lett. 325 (2000) 171–175.
[7] M. Rini, A. Kummrow, J. Dreyer, E.T.J. Nibbering, T. Elsaesser, Faraday Discuss. 122 (2002) 27–40.
[8] S. Lochbrunner, A.J. Wurzer, E. Riedle, J. Phys. Chem. A 107 (2003) 10580–10590.
[9] R. de Vivie-Riedle, V. De Waele, L. Kurtz, E. Riedle, J. Phys. Chem. A 107 (2003) 10591–10599.
[10] S. Lochbrunner, K. Stock, E. Riedle, J. Mol. Struct. 700 (2004) 13–18.
[11] M. Ziółek, J. Kubicki, A. Maciejewski, R. Naskręcki, A. Grabowska, Phys. Chem. Chem. Phys. 6 (2004) 4682–4689.
[12] T. Rosenfeld, M. Ottolenghi, A.Y. Meyer, Mol. Photochem. 5 (1973) 39–60.
[13] P.F. Barbara, P.M. Rentzepis, L.E. Brus, J. Am. Chem. Soc. 102 (1980) 2786–2791.
[14] K. Kownacki, Ł. Kaczmarek, A. Grabowska, Chem. Phys. Lett. 210 (1993) 373–379.
[15] K. Kownacki, A. Mordziński, R. Wilbrandt, A. Grabowska, Chem. Phys. Lett. 277 (1994) 270–276.
[16] M.I. Knyazhansky, A.V. Metelitsa, A.Ya. Bushkov, S.M. Aldoshin, J. Photochem. Photobiol. A 97 (1996) 121–126.
[17] S. Mitra, N. Tamai, Chem. Phys. Lett. 282 (1998) 391–397.
[18] N. Otsubo, Ch. Okabe, H. Mori, K. Sakota, K. Amimoto, T. Kawato, H. Sekiya, J. Photochem. Photobiol. A 154 (2002) 33–39.
[19] M.Z. Zgierski, A. Grabowska, J. Chem. Phys. 112 (2000) 6329–6337.
[20] M. Ziółek, J. Kubicki, A. Maciejewski, R. Naskręcki, A. Grabowska, Chem. Phys. Lett. 369 (2003) 80–89.
[21] A. Grabowska, K. Kownacki, J. Karpiuk, S. Dobrin, Ł. Kaczmarek, Chem. Phys. Lett. 267 (1997) 132–140.
[22] A. Mordziński, A. Grabowska, W. Kühnle, A. Krówczyński, Chem. Phys. Lett. 101 (1983) 291–296.
[23] U. Brackmann, N.P. Ernsting, D. Ouw, K. Schmitt, Chem. Phys. Lett. 110 (1984) 319–324.
[24] N.P. Ernsting, J. Am. Chem. Soc. 107 (1985) 4564–4565.
[25] A. Mordziński, W. Kühnle, J. Phys. Chem. 90 (1986) 1455–1458.
[26] A. Grabowska, A. Mordziński, N. Tamai, K. Yoshihara, Chem. Phys. Lett. 153 (1988) 389–392.
[27] B. Dick, Chem. Phys. Lett. 158 (1989) 37–44.
[28] A. Grabowska, A. Mordziński, N. Tamai, K. Yoshihara, Chem. Phys. Lett. 169 (1990) 450–456.
[29] J. Sepioł, Chem. Phys. Lett. 175 (1990) 419–424.
[30] A. Grabowska, A. Mordziński, K. Kownacki, E. Gilabert, C. Rullière, Chem. Phys. Lett. 177 (1991) 17–22.
[31] A. Grabowska, J. Sepioł, C. Rullière, J. Phys. Chem. 95 (1991) 10493–10495.
[32] N.P. Ernsting, Th. Arthen-Engeland, M.A. Rodriguez, W. Thiel, J. Chem. Phys. 97 (1992) 3914–3919.
[33] A. Mühlpfordt, U. Even, N.P. Ernsting, Chem. Phys. Lett. 263 (1996) 178–184.
[34] R. Wortmann, S. Lebus, H. Reis, A. Grabowska, K. Kownacki, S. Jarosz, Chem. Phys. 243 (1999) 295–304.
[35] N.P. Ernsting, S.A. Kovalenko, T. Senyushkina, J. Saam, V. Farztdinov, J. Phys. Chem. A 105 (2001) 3443–3453.
[36] J. Weiβ, V. May, N.P. Ernsting, V. Farztdinov, A. Mühlpfordt, Chem. Phys. Lett. 346 (2001) 503–511.
[37] E. Luzina, J.M. Kauffman, A. Mordziński, Chem. Phys. Lett. 400 (2004) 1–6.
[38] M. Milewski, W. Augustyniak, A. Maciejewski, J. Phys. Chem. A 102 (1998) 7427–7434.
[39] S.R. Meech, D. Philips, J. Photochem. 23 (1983) 193–217.
[40] T. Wróżowa, B. Ciesielska, D. Komar, J. Karolczak, M. Maciejewski, J. Kubicki, Rev. Sci. Instrum. 75 (2004) 3107–3121.
[41] A. Maciejewski, R. Naskręcki, M. Lorenc, M. Ziółek, J. Karolczak, J. Kubicki, M. Matysiak, M. Szymański, J. Mol. Struct. 555 (2000) 1–13.
[42] T. Nakayama, Y. Amijima, K. Ibuki, K. Hamanoue, Rev. Sci. Instrum. 68 (1997) 4364–4371.
[43] M. Ziółek, M. Lorenc, R. Naskręcki, Appl. Phys. B 72 (2001) 843–847.
[44] M. Lorenc, M. Ziółek, R. Naskręcki, J. Karolczak, J. Kubicki, A. Maciejewski, Appl. Phys. B 74 (2002) 19–27.
[45] R.S. Fee, M. Maroncelli, Chem. Phys. 183 (1994) 235–247.
[46] D. Zhong, A. Douhal, A.H. Zewail, Proc. Natl. Acad. Sci. U.S.A. 97 (2000) 14056–14061.
[47] A. Douhal, T. Fiebig, M. Chachisvilis, A.H. Zewail, J. Phys. Chem. A 102 (1998) 1657–1660.